Journal of Geophysical Research: Atmospheres

RESEARCH ARTICLE
10.1029/2018JD028820

Parameterized Vertical Concentration Profiles for Aerosols in the Marine Atmospheric Boundary Layer

Indrajith D. Nissanka[1], Hyungwon John Park[1], Livia S. Freire[2], Marcelo Chamecki[3], Jeffrey S. Reid[4], and David H. Richter[1]

[1]Department of Civil and Environmental Engineering and Earth Sciences, University of Notre Dame, IN, Notre Dame, USA, [2]Graduate Program in Environmental Engineering, Federal University of Parana, Curitiba, Brazil, [3]Department of Atmospheric and Oceanic Sciences, University of California, Los Angeles, CA, USA, [4]U.S. Naval Research Laboratory, Monterey, CA, USA

Key Points:
- A new 1-D model shows that particle concentrations in marine atmospheric boundary layer depend heavily on particle size and turbulence level
- Linear net vertical flux profile in the mixed layer is essential for accurate prediction of concentration profiles above the surface layer

Correspondence to:
D. H. Richter,
David.Richter.26@nd.edu

Citation:
Nissanka, I. D., Park, H. J., Freire, L. S., Chamecki, M., Reid, J. S., & Richter, D. H. (2018). Parameterized vertical concentration profiles for aerosols in the marine atmospheric boundary layer. *Journal of Geophysical Research: Atmospheres*, *123*. https://doi.org/10.1029/2018JD028820

Received 12 APR 2018
Accepted 29 AUG 2018
Accepted article online 3 SEP 2018

Abstract Information about sea spray aerosol particle transport and their vertical distribution in the marine atmospheric boundary layer (MABL) is important in marine meteorological forecasting and geobiochemical models. However, due to difficulties in field observations, values of aerosol concentration are often limited to point measurements, and obtaining the size-resolved concentration profiles is quite challenging. Hence, numerical and analytical studies are vital in modeling the transport of aerosols in the atmospheric boundary layer and beyond. Due to their coarse resolution, most mesoscale and global aerosol models do not accurately resolve the sea spray and aerosol concentrations in the MABL, especially in the surface layer. The objective of the present study is to develop a relatively simple, one-dimensional analytical model to calculate concentration profiles of aerosols in the MABL. In this study, a new analytical model relating surface flux to vertical concentration profile in the MABL is proposed. The model accounts for the different atmospheric stability and particle settling velocity, thus providing size-resolved vertical profiles of aerosol concentration. The equations developed here extend the surface layer similarity models to the mixed layer. Model results are compared to aerosol concentration profiles emitted from a surface source obtained from large eddy simulations, for both neutral and unstable atmospheric stability and for particle sizes ranging from 1 to 30 μm. Though the model is developed for sea spray aerosols, it can be used to calculate vertical concentration profiles for other types of settling particles, including dust and sand particles in the atmospheric boundary layer.

1. Introduction

Sea spray and sea salt particles make up a significant fraction of the aerosols suspended in the atmosphere and represent approximately 90% of the aerosols in the marine atmospheric boundary layer (MABL; Lewis & Schwartz, 2004; Seinfeld & Pandis, 1998; Veron, 2015). These marine aerosol particles are generated across a wide span of sizes through several different mechanisms at the sea surface, including bubble bursting with film and jet drops, splashing, and mechanical tearing from waves (Andreas et al., 1995; Veron, 2015). After emission at the surface, the vertical distribution of sea spray aerosols throughout the MABL is largely dictated by the balance between the atmospheric turbulence and particle settling due to gravity. Depending on the size and injection, individual sea spray droplets can remain in the atmosphere for few seconds to several weeks, impacting atmospheric boundary layer processes ranging from local to global scales (Veron, 2015). This includes their important role in affecting radiative transfer both directly (Kleefeld et al., 2002) and indirectly (Twohy et al., 2005). Sea spray droplets and aerosols also interact with various trace gases in the atmosphere. Hence, their distribution is important in understanding atmospheric chemistry, as well as airborne geochemical, organic, and biological processes (O'Dowd & De Leeuw, 2007). Thus, characterizing the transport of marine aerosol particles and their vertical distribution throughout the MABL can be important for accurate marine meteorological forecasting and atmospheric biogeochemical modeling. The difficulty, however, with most global and even many mesoscale forecasting models is that the MABL remains unresolved at key boundaries, and thus, the vertical variability and steep gradients of aerosol concentration throughout the MABL cannot be explicitly represented.

Due to the practical challenges in making field observations, measurements of size-resolved marine spray aerosol concentrations are oftentimes limited to single heights near the surface (e.g., from a tower, Smith et al., 1993; ship, de Leeuw, 1986; or buoy, Norris et al., 2013). Aircraft measurements have been employed to measure vertical aerosol distributions (Blanchard et al., 1984; Lenain & Melville, 2017; Reid et al., 2001), including a few observations close to the surface; however, near-surface observations (less than roughly 30 m depending on sea state) are often difficult and issues with reliable and consistent particle count statistics across measurement devices persist (Reid et al., 2006). Other methods based on remote sensing, including lidar-based backscatter retrievals or Doppler radar (Fairall et al., 2014), have been used but suffer from calibration uncertainties and low spatial resolution. Thus, a size-resolved vertical concentration profile with consistent sampling between the bottom, middle, and top throughout the entirety of the MABL is a difficult quantity to characterize based on field observations alone, especially when attempting to understand its dependence on meteorological conditions such as wind speed or atmospheric stability. This uncertainty then feeds the high variability in inferred spray aerosol production flux estimates, which span a wide range in the literature (Andreas, 1998; de Leeuw et al., 2011; Lewis & Schwartz, 2004; O'Dowd & De Leeuw, 2007).

As a result, numerical and theoretical efforts can help fill the gaps in understanding aerosol transport and distribution in the MABL. In this regard, large eddy simulation (LES) has emerged as a valuable tool for studying boundary layer turbulence and scalar transport (Bou-Zeid et al., 2005; Moeng, 1984; Moeng & Sullivan, 1994; Porté-Agel, 2004). Within the LES context, particle and aerosol dispersion can be then treated from either an Eulerian (Chamecki & Meneveau, 2011; Pan et al., 2013) or Lagrangian (Weil, 1990; Weil et al., 2004) point of view. In the former, scalars are treated as a continuous field on the computational grid (Chamecki et al., 2009), while in the latter, aerosols are treated as Lagrangian point particles that are advected and dispersed by the local velocity interpolated from the LES computational mesh. Other numerical methodologies, including direct numerical simulation (DNS) and Lagrangian stochastic models, have been utilized for studying spray aerosol processes in the MABL as well (Mueller & Veron, 2010, 2009; Peng & Richter, 2017; Richter & Chamecki, 2018). The goal of these techniques is to accurately resolve turbulence in ways unattainable on coarse global- or regional-scale model grids, then to use this information to better parameterize unresolved turbulent transport processes in the MABL.

While much work has been done to characterize the turbulent transport of passive scalars in the boundary layer, for instance, the so-called top-down and bottom-up diffusion model, which recognizes the asymmetry of vertical velocity variance and scalar flux in the convective boundary layer (Moeng & Wyngaard, 1984; Wyngaard & Brost, 1984), the evolution of aerosol concentration can be complicated by their gravitational settling. As a result, the concentration at any height reflects the competition between the upward turbulent flux (if the source is located at the ground) and the downward settling flux. Focusing only on the steady, horizontally homogeneous surface layer, the vertical profile of passive scalar concentration follows the well-known Monin-Obukhov (MO) similarity theory, which yields a logarithmic profile in neutral stability (Monin & Yaglom, 1971). If the scalar is given a constant settling velocity, then instead of a logarithmic vertical distribution, the concentration in a neutral surface layer can be described by the classic power law distribution (Prandtl, 1953; Rouse, 1937), whose power depends on settling velocity. While the latter theory assumes a steady state balance between settling and turbulence (i.e., zero surface net flux), the existence of a true, steady equilibrium solution has been questioned especially for small suspended particles (Hoppel et al., 2002; Xiao & Taylor, 2002). The theory can be extended to include a constant net flux (either emission or deposition) that reflects an imbalance between the two—a more realistic situation seen in the MABL (Chamberlain, 1967; Hoppel et al., 2002; Kind, 1992). The influence of atmospheric stability can be included in this model as well (Chamecki et al., 2007; Freire et al., 2016). Furthermore, these models can be extended to obtain self-similarity solution for concentration profile in steady state two-dimensional particle transport with horizontal advection (Chamecki & Meneveau, 2011; Zhu et al., 2017).

While these studies focus almost exclusively on the atmospheric surface layer, the objective of the present study is to extend this theory in order to provide a simple parameterization for the concentration profile of settling marine aerosols in the entire MABL. Having such a model, which can take into account various particle sizes, will benefit large-scale regional and global models, which do not have sufficient resolution to resolve transport in the boundary layer and will help interpret field observations where vertical gradients of concentration are large and where measurements are scarce or at coarse resolution.

2. Model Formulation

The aim of the present study is to extend existing theories that model the vertical concentration profiles of aerosol particles in the surface layer throughout the entire MABL. The new theoretical model accounts for both atmospheric stability and gravitational settling and closely follows the surface layer concentration profile for dust particles developed by Freire et al. (2016). Several modifications are introduced to extend the theory to the full mixed layer, while the surface layer behavior is retained. Here *mixed layer* refers to the layer above the surface layer, which is bounded by the temperature inversion layer at the top of the boundary layer. The surface layer height is roughly $0.1z_i$, where z_i is the inversion layer height.

We start with the advection-diffusion equation for passive scalars, given by

$$\frac{\partial C}{\partial t} + \frac{\partial (v_i C)}{\partial x_i} = \frac{\partial}{\partial x_i}\left(D_c \frac{\partial C}{\partial x_i}\right), \tag{1}$$

where C is the instantaneous concentration of aerosols, D_c is molecular diffusivity of particle concentration, t is time, and x_i represents the three coordinate directions(x, y, z). The concentration C is advected by a velocity v_i, which is equal to the local fluid velocity u_i for the case passive, nonsettling scalars. Following the original work of Prandtl (1953) and Rouse (1937), a constant gravitational settling velocity is added to account for particle settling:

$$v_i = u_i - w_s \delta_{i3}, \tag{2}$$

where δ_{i3} is the Kronecker delta and $w_s = g d_p^2 \rho_p / (18\mu_f)$ is the Stokes terminal velocity of a spherical particle of density ρ_p and diameter d_p in a fluid of viscosity μ_f (Balachandar & Eaton, 2010). Thus, the advection velocity is simply a combination of the local fluid velocity and a constant gravitational settling velocity. Additional corrections to v_i can be made for particle inertia as well (Maxey, 1987; Richter & Chamecki, 2018).

Assuming horizontal homogeneity with no mean vertical air velocity and neglecting molecular diffusion (the molecular diffusion is negligible compared to the turbulent fluxes), decomposing the velocity and concentration into their horizontal mean and fluctuation (i.e., $C = \bar{C} + c'$) in equation (1) yields an expression for the horizontally averaged concentration $\bar{C}$ as a function of time:

$$\frac{\partial \bar{C}}{\partial t} - w_s \frac{\partial \bar{C}}{\partial z} + \frac{\partial \overline{w'c'}}{\partial z} = 0, \tag{3}$$

where $\overline{w'c'}$ is the vertical turbulent flux of aerosols and z is the height from the surface.

Integrating equation (3) over the vertical coordinate from a lower reference height z_r to an arbitrary height z yields

$$\int_{z_r}^{z} \frac{\partial \bar{C}}{\partial t} dz' + \overline{w'c'} - w_s \bar{C} = \left[\overline{w'c'} - w_s \bar{C}\right]_{z=z_r} \equiv \Phi. \tag{4}$$

Here as in previous studies (Freire et al., 2016; Kind, 1992), Φ represents an integration constant whose physical meaning is the net difference between the turbulent and settling fluxes at the lower reference height z_r. Rearranging the equation, we define the net vertical flux at any height z as

$$q_{\text{net}}(z) = \overline{w'c'} - w_s \bar{C} = \Phi - \int_{z_r}^{z} \frac{\partial \bar{C}}{\partial t} dz, \tag{5}$$

where $q_{\text{net}}(z_r)$ is equal to Φ, the net flux at the near-surface reference height z_r.

Equation (5) indicates that the net vertical flux at any height can be interpreted either as a local balance of gravitational settling and turbulent flux (first equality), or as a modified surface flux, which depends on the time rate of change of $\bar{C}$ (second equality). Often, for simplicity, an assumption is made that the concentration $\bar{C}$ is steady in time (Andreas et al., 2010; Fairall et al., 2009; Veron, 2015), which according to equation (5) is equivalent to saying that the gravitational settling flux is in balance with the turbulent flux. In the surface layer this approximation is appropriate, as demonstrated by Freire et al. (2016), because the unsteady term $\frac{\partial \bar{C}}{\partial t}$ becomes negligible after a short period of time, even before the overall MABL has been fully loaded with aerosol mass. Over the entire MABL, however, it takes much longer for the concentration to achieve a steady state and for the fluxes to balance each other (Hoppel et al., 2002). In this situation, the approximation $\frac{\partial \bar{C}}{\partial t} \approx 0$ does not hold any longer. Hence, by extending the vertical concentration profile into the mixed layer, we can no longer neglect the unsteady term in equation (5). For a passive scalar, Wyngaard and Brost (1984) showed that the curvature for the scalar flux profile is caused only by the time change in the mean scalar gradient and

that if the temporal change in the scalar gradient is assumed to be negligible, then the flux profile is linear with height. Based on this idea, in the current model formulation, we assume that throughout the MABL, $\frac{\partial \bar{C}}{\partial t} = \beta$ (a constant), which results in a linear profile for net vertical flux q_{net} with height, that is,

$$q_{\text{net}} = \Phi - \int_{z_r}^{z} \frac{\partial \bar{C}}{\partial t} \mathrm{d}z = \Phi - \beta z. \tag{6}$$

Substituting equation (6) into equation (5) and invoking K theory (gradient diffusion hypothesis) for the turbulent flux $\overline{w'c'}$ in terms of an eddy diffusivity K_c, equation (5) becomes

$$-K_c \frac{\mathrm{d}\bar{C}}{\mathrm{d}z} - w_s \bar{C} = \Phi - \beta z. \tag{7}$$

The right-hand side of equation (7) represents the net vertical flux q_{net}, which is now changing linearly with height, where again Φ represents the net surface flux, defined as the imbalance between the particle emission and the deposition at the surface. Since, for the cases of interest here, aerosol particles are emitted from the surface, the maximum net vertical flux should be at the surface. If we then further assume that the net vertical flux reaches zero at the top of the boundary layer, then the gradient of the linear flux profile β can be expressed as $\beta = \Phi / z_i$. Here z_i is the height of the MABL as measured by the maximum temperature gradient, although this assumption may not be accurate if the particles are allowed to disperse into the inversion layer, especially for strongly unstable stratification. This issue will be addressed in section 4.1.

To close equation (7), the eddy diffusivity profile K_c needs to be defined throughout the entire MABL. There are well-known and accepted formulas, which can be used to specify the height dependency of K_c in the surface layer (constant-flux layer). Assuming that the particle eddy diffusivity is equal to the momentum diffusivity in the surface layer, MO similarity theory states that eddy diffusivity is of the form $K_c = \kappa u_* z$, where κ is the von Kármán constant and u_* is the friction velocity. This is a good approximation under neutral stability to calculate the concentration profile in the surface layer (Kind, 1992). However, a significant increase in transport can occur under unstable conditions (Freire et al., 2016). To account for stability, the dimensionless total vertical flux of particles can be expressed as a function of dimensionless stability parameter $\zeta = z/L$, where $L = -u_*^3 \bar{\theta}_s / (\kappa g \overline{w'\theta'}_s)$ is the Obukhov length, $\bar{\theta}_s$ and $\overline{w'\theta'}_s$ are the temperature and sensible heat flux at the surface, respectively, and g is acceleration of gravity (Monin & Yaglom, 1971; Wyngaard, 2010). Thus, a more general form of the eddy diffusivity can be expressed by incorporating atmospheric stability as (Freire et al., 2016; Kaimal & Finnigan, 1994; Shao, 2000):

$$K_c = \frac{\kappa u_* z}{\phi_c(\zeta)}, \tag{8}$$

where $\phi_c(\zeta)$ is a stability function. Freire et al. (2016) used a similarity function for passive scalars given by Kaimal and Finnigan (1994),

$$\phi_c(\zeta) = \begin{cases} (1 - 16\zeta)^{-1/2}, & \text{if } \zeta < 0 \text{ (unstable)}, \\ 1 + 5\zeta, & \text{if } \zeta > 0 \text{ (stable)}, \\ 1, & \text{if } \zeta = 0 \text{ (neutral)}. \end{cases} \tag{9}$$

The eddy diffusivity defined by equation (8) is only valid for the surface layer. In the mixed layer, defining K_c is not as clear, particularly for numerical models (Troen & Mahrt, 1986). Several approaches have been used in the literature to define the eddy diffusivity profile, such as linearly decreasing from the surface layer to top of the boundary layer (Estoque, 1963), exponentially decreasing with height from the surface layer (McPherson, 1968), and by finding an interpolating polynomial passing through prescribed points with predefined slopes (O'Brien, 1970). However, the general approach for approximating the eddy diffusivity in the mixed layer has used a power law dependence on z/z_i, and scale parameters were derived from similarity theory or empirically. A commonly used shape function is of the form (Brost & Wyngaard, 1978; Troen & Mahrt, 1986)

$$K_c = u_* \phi_c^{-1} \kappa z \left(1 - \frac{z}{z_i}\right)^p, \tag{10}$$

where z_i is the inversion layer height. The exponent $p = 2$ has been commonly used in the literature, while values between 2 and 3 agree with different observed profiles. In the present study, we use an eddy diffusivity in the mixed layer as a cubic power (i.e., $p = 2$) of height z. However, to be consistent with previous surface

layer similarity theories, we make the eddy diffusivity profile linear with z up to the surface layer, then transitioning into a cubic profile. Hence, we use a combination of both equations (8) and (10) to define the eddy diffusivity, which is given by

$$K_c(z) = \begin{cases} \frac{\kappa u_* z}{\phi_c(\zeta) Sc}, & \text{if} z < z_b, \\ \frac{a\kappa u_* z\left(1-\frac{z}{z_i}\right)^2}{\phi_c(\zeta) Sc}, & \text{if} z \geq z_b, \end{cases} \tag{11}$$

where z_b is the surface layer height, which is taken as 10% of the boundary layer height, κ is taken as $\kappa = 0.41$, Sc is the turbulent Schmidt number, and the constant $a = 1/(1 - z_b/z_i)^2$ is used to make sure that the K_c transition from the surface layer to the mixed layer is continuous. Because there is no well-defined parameterization of $\phi_c(\zeta)$ for the mixed layer, the surface layer formulation given by equation (9) is adopted throughout the entire MABL in the present study. With this approach, turbulent mixing reaches zero at the top of the boundary layer. This condition should be relaxed if the model allows mixing above the boundary layer (Troen & Mahrt, 1986). More details about how to address this issue at the top of the boundary layer is discussed in section 4.1.

Finally, a closed, first-order differential equation for $\bar{C}$ can be written as follows:

$$\frac{d\bar{C}}{dz} = -\frac{1}{K_c}[w_s\bar{C} + \Phi - \beta z]. \tag{12}$$

Given the aforementioned expression for K_c, equation (12) does not permit an analytic formula for $\bar{C}(z)$. Therefore, in section 4 where LES results are compared to the one-dimensional model, we present numerical solutions to equation (12) using standard integration techniques. In section 4.3, we revisit the possibility of formulating an analytic solution to equation (12). We also note that strictly speaking, $\bar{C}$ is a function of both t and z, but we have implicitly incorporated the time dependence as a tendency term into an expression for $\bar{C}(z)$ that is valid only locally in time. In the comparisons below, all apparent time variation results solely from time-dependent boundary conditions (i.e., surface concentrations) retrieved from LES.

3. Large Eddy Simulations

Due to the difficulty in obtaining surface emission fluxes and given the wide range of droplet size variations in the existing field observations, observational validation of the model is difficult. For instance, previous attempts to fit the value of the surface flux and compare models with measurements did not yield conclusive results (Chamecki et al., 2007). Thus, in the absence of adequate observational data to compare the mean vertical profile, LES results are used to validate the newly developed model and the assumptions made during the derivation process.

3.1. Numerical Details

The LES code used here solves the three-dimensional filtered momentum equations in a rotating frame of reference, using a fully dealiased pseudo-spectral method in the horizontal directions and a second-order centered finite-difference method in the vertical direction. Time integration is performed by a fully explicit second-order Adams-Bashforth scheme. The subgrid-scale model corresponds to the scale-dependent, Lagrangian-averaged dynamic Smagorinsky model described by Bou-Zeid et al. (2005). Particles are simulated as a concentration field using a finite-volume scheme based on a filtered advection-diffusion equation with an additional term to represent gravitational settling. More details about the LES model can be found in Bou-Zeid et al. (2005), Kumar et al. (2006), and Freire et al. (2016).

In the simulation presented here, the flow is driven by a constant mean pressure gradient force in geostrophic balance above the MABL. Boundary conditions are periodic in the horizontal directions and stress free at the top of the domain. Bottom boundary conditions are given by MO similarity theory for horizontal components of velocity, and a zero vertical velocity is imposed at the ground based on a staggered grid approach. Surface fluxes for temperature and particle concentration are imposed, and the surface is assumed flat with a constant aerodynamic roughness.

3.2. Simulation Setup

The simulation setup used in this study corresponds to the emission cases of Freire et al. (2016). Domain size and number of grid points are 3,000 × 3,000 × 1,000 m ($x \times y \times z$) and 160 × 160 × 320, respectively. In all

Table 1
Simulation Setup: Physical Parameters

Parameter	Neutral (N)	Strongly unstable (Un-S)	Weakly unstable (Un-W)
(U_g, V_g) (m/s)	(16,0)	(10,0)	(10,0)
$\overline{w'\theta'}_s$ (K m/s)	0.0	0.24	0.05
u_* (m/s)	0.4	0.4	0.35
L (m)	$-\infty$	−20	−62
$z_{i,0}$ (m)	570	570	570
$z_{i,f}$ (m)	570	600	590

Note. $z_{i,0}$ and $z_{i,f}$ are the initial and final height of the MABL in the simulations, respectively, (U_g, V_g) are the geostrophic wind, $\overline{w'\theta'}_s$ is the surface heat flux, and u_* is the friction velocity. MABL = marine atmospheric boundary layer.

simulations the MABL is topped with a strong temperature inversion of 0.1 K/m to restrict the growth of the MABL. The aerodynamic roughness length is set to $z_0 = 0.001$ m, and a net particle flux of $\Phi = 0.2\ \mu g \cdot m^{-2} \cdot s^{-1}$ is used. Simulations were performed separately for particles diameters of 1, 10, 20, and 30 μm driven by the same velocity field. Neutral and unstable cases were performed with the parameters presented in Table 1. For the neutral case the MABL height remains approximately constant throughout the simulation, whereas for unstable cases a small increase in MABL height is observed.

All simulations were first run without particles for a period corresponding to approximately 3 hr in the neutral and 1 hr in the unstable simulations, to allow the turbulence to spin-up and reach steady state conditions. The aerosol concentrations are initialized with zero concentration in the entire domain. More details about the simulations and setup can be found in Freire et al. (2016).

4. Results and Discussion

The key modifications made to extend the surface layer model of Freire et al. (2016) to the current model for the full boundary layer are (1) the eddy diffusivity profile given in equation (11), where we assume that the turbulent eddy diffusivity can be represented by a cubic function of height and (2) the linear net vertical flux profile given by equation (6), which represents unsteadiness in the integrated particle loading throughout the MABL. Before using the proposed model to calculate mean concentration profiles, the validity of these assumptions is tested by comparing them with the LES results. In Figure 1, the normalized eddy diffusivity profile calculated from equation (11) is presented. The comparison for neutral atmospheric stability is also given in Figure 1a, which depicts a good agreement between LES simulation results and that predicted by equation (11). Near-infinite gradients of the mean concentration profile in the unstable cases prevents a straightforward calculation of an effective K_c from the LES profiles. However, the selected eddy diffusivity

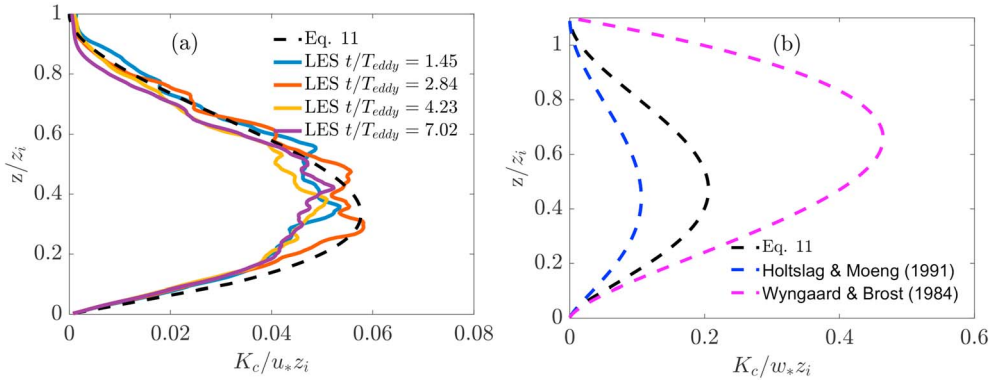

Figure 1. Normalized eddy diffusivity profiles calculated from equation (11) for (a) neutral atmospheric stability (case N), compared to effective K_c calculated from the large eddy simulation (LES), (b) unstable stratification (case Un-S and Un-W) compared to Wyngaard and Brost (1984) and Holtslag and Moeng (1991) bottom-up eddy diffusivity. w_* is the convective velocity scale.

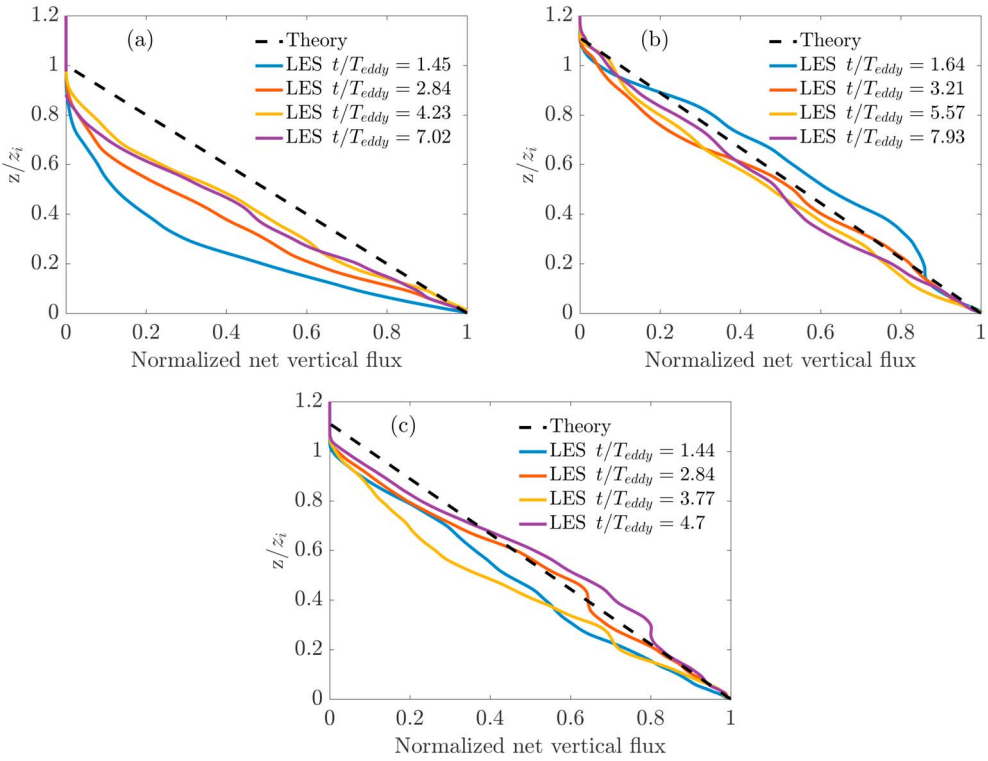

Figure 2. Net vertical flux of aerosols normalized by the surface flux for 10 μm particles in the (a) neutral atmospheric boundary layer, (b) unstable atmospheric boundary layer (case Un-S), and (c) unstable atmospheric boundary layer (case Un-W). *Theory* indicates the linear approximation. LES = large eddy simulation.

model for unstable cases yields K_C values that are similar in shape and range to the established models of Holtslag and Moeng (1991) and Wyngaard and Brost (1984).

Another simplification of the model is the assumption that the unsteady term in equation (3) is constant throughout the mixed layer (i.e., $\frac{\partial \bar{C}}{\partial t} = \beta$). This leads to a net vertical flux that changes linearly with the height from surface z (given in equation (6). To test the validity of this assumption, the net vertical scalar flux is compared with the LES results. The net vertical flux is calculated as a sum of the resolved and subfiltered scalar fluxes and subtracting the gravitational settling flux $w_s\bar{C}$. Figure 2 illustrates the comparison of net vertical flux profile normalized by the net surface flux for both neutral and unstable atmospheric stability. It is seen from Figures 2b and 2c that for any degree of unstable stratification, approximating the total vertical flux of concentration as a linear function of height is a valid assumption; this linearity establishes quickly in time. When nondimensionalized by an eddy turnover time, the fluxes become approximately linear after roughly T_{eddy}. The eddy turnover time for neutral case is defined as $T_{\text{eddy}} = z_i/u_*$ and for unstable simulations $T_{\text{eddy}} = z_i/w_*$, where w_* is the convective velocity scale calculated as $w_* = \left(\frac{g}{T_s} z_i \overline{w'\theta'}_s\right)^{1/3}$, $T_s = 274$ K (the surface temperature).

Figure 2a shows that the linear approximation for the total flux does not hold as strongly for neutral stratification. Furthermore, the flux profile develops much more slowly for neutral stratification, which is expected given the lower degree of vertical mixing compared to unstable stratification (even weak unstable stratification). From the flux profiles and K_c profiles of Figures 2 and 1, respectively, we anticipate that the assumptions behind the model given by equation (12) are sufficiently justified, particularly for unstable stratification.

4.1. Flux Correction at the Inversion Layer

Based on the LES results for unstable atmospheric stability, the net vertical flux does not identically approach zero at the inversion height z_i (as computed by the maximum temperature gradient). A similar situation is observed by Waggy et al. (2013), where they found significant viscous and turbulent fluxes at the inversion height. Based on DNS they found that the total flux reaches zero at $z/z_i \approx 1.13$. The relative significance of the flux at the inversion layer height depends on the rate at which the inversion layer is growing and the way in

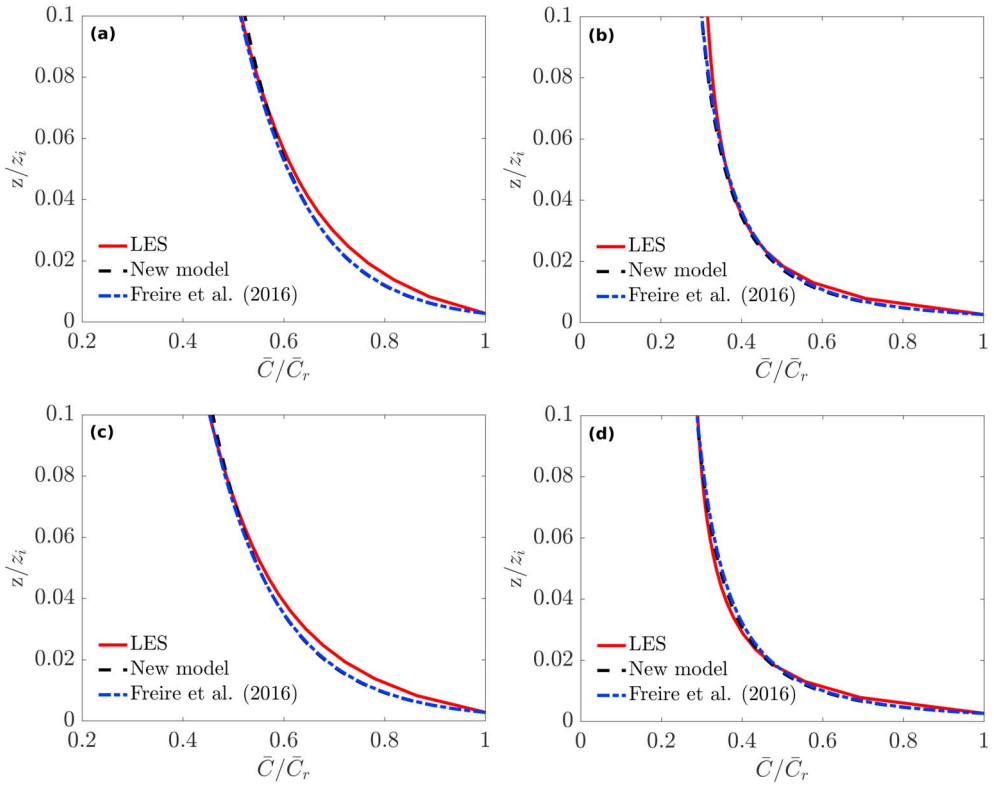

Figure 3. Comparison of the normalized mean vertical concentration profile in the surface layer for the representative cases of (a) 1-μm particles for case N; (b) 1-μm particles for case Un-S; (c) 10-μm particles for case N; and (d) 10-μm particles for case Un-S. $\bar{C}_r$ is taken as the concentration at the first vertical grid point from the large eddy simulation (LES) simulation (1.56 m).

which the boundary layer height is determined. To consider this in the current model formulation, we assume that there is a vertical flux into the inversion layer at the top (i.e., the net vertical flux is nonzero at z_i). Following the bottom-up and top-down diffusion approach by Wyngaard and Brost (1984), we consider the surface flux and the flux at the inversion layer as two separate fluxes. However, in the present model formulation the flux at the top is considered as an advective flux going out from the MABL instead of a top-down diffusion. The net vertical flux is therefore calculated as the superposition of the two fluxes as $\Phi + \Phi_t$, where Φ_t is the flux going out at the inversion layer. Combining this with our original assumption where the net vertical flux varies linearly with height, we can modify the net vertical flux given in equation (6) as

$$q_{\text{net}}(z) = \Phi(1 - z/z_i) + \Phi_t(z/z_i). \tag{13}$$

We represent the inversion layer flux at the top as a fraction of the surface flux, that is, $\Phi_t = \alpha\Phi$. Then the net vertical flux can be expressed as

$$q_{\text{net}}(z) = \Phi\left(1 - (1 - \alpha)z/z_i\right). \tag{14}$$

This modified net vertical flux relation given by equation (14) can be used to replace the right-hand side of equation (7) in order to calculate the mean concentration profile. Figures 2b and 2c show the comparison of the net vertical flux calculated from equation (14) with the LES results for the unstable ABL. Often, $\alpha \approx 0.2$ is used for heat and water vapor; however, here we use $\alpha = 0.1$ based on LES results. The LES simulations use a strong temperature inversion at the top of the MABL, and the scalar field experiences gravitational settling, which apparently cause α to be slightly smaller than the typical values. Then, net vertical flux profile given in equation (14) can be used to approximate the net vertical flux profile in the mixed layer.

Furthermore, near the top of the boundary layer, the turbulent diffusivity profile determines the importance of the flux at the inversion layer. The turbulent diffusivity calculated from equation (11) reaches zero at the

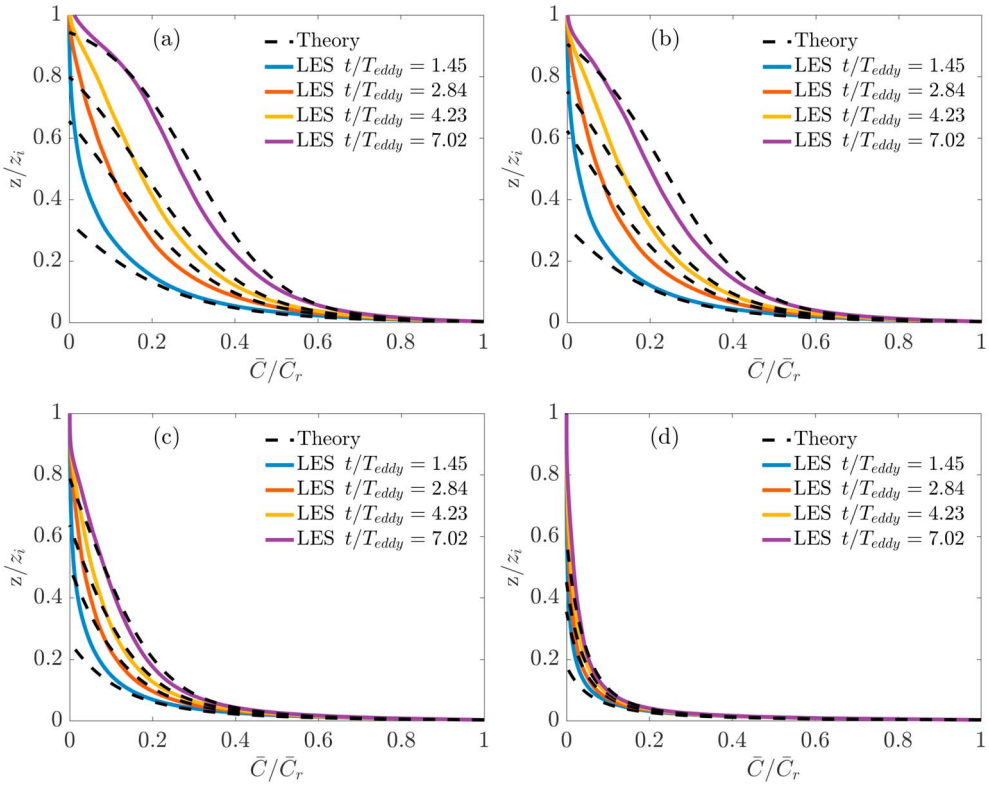

Figure 4. Comparison of normalized mean vertical concentration profile with simulation results from large eddy simulation (LES) for case N: (a) 1-μm particles, (b) 10-μm particles, (c) 20-μm particles, and (d) 30-μm particles. $\bar{C}_r$ is taken as the concentration at the first vertical grid point from the LES simulation (1.56 m).

inversion layer height. However, in unstable atmospheric conditions, to be consistent with the upwards flux discussed above, we extended the diffusivity profile beyond the inversion layer by assuming that K_C also approaches zero at $1.1z_i$.

4.2. Comparison of the Mean Vertical Concentration Profile With LES Simulations

The mean vertical concentration profile calculated by solving equation (12) is compared with the LES results. The parameters needed to solve equation (12) (u_*, z_i, L) were obtained from the LES and were kept as constants for different particle diameters. The value obtained at the end of the simulation for the inversion layer height ($z_{i,f}$), provided in Table 1, is used as z_i for the calculation. In addition, due to the different numerical approaches used for vertical advection of momentum and scalar concentration in the LES, a turbulent Schmidt number ($Sc = 1.3$) is introduced to the theoretical profile for comparison. To calculate the time evolution of concentration profile it is required to input a reference concentration ($\bar{C}_r$) to the model; for the present calculations $\bar{C}_r$ is taken as the concentration at the first vertical grid point from the LES simulation (i.e., $z_r = 1.56m$). In field conditions this value would be taken as a point measurement of concentration at a known reference height.

Before using the model to calculate concentration profiles in the full MABL, it is important to show that the new model can reproduce the surface layer concentration profiles. Hence, concentration profiles calculated from the model in the surface layer are compared with LES simulations and are given in Figure 3. In addition, these are compared to the original surface layer formula by Freire et al. (2016). It is evident from Figure 3 that the current model indeed reproduces the concentration profile in the surface layer compared to the LES and is consistent with the previous surface layer models in the literature (Freire et al., 2016; Kind, 1992). Within the surface layer, the key difference between the new model and that of Freire et al. (2016) is that the new model assumes that the net vertical scalar flux is changing linearly with height, while Freire et al. (2016) assumed it to be constant in the surface layer. Based on Figure 3, the two models give almost identical results, suggesting that the linear correction to the net vertical flux has a negligible effect within the surface layer. This confirms the finding of Freire et al. (2016) that the equilibrium assumption (i.e., balance between turbulent flux and

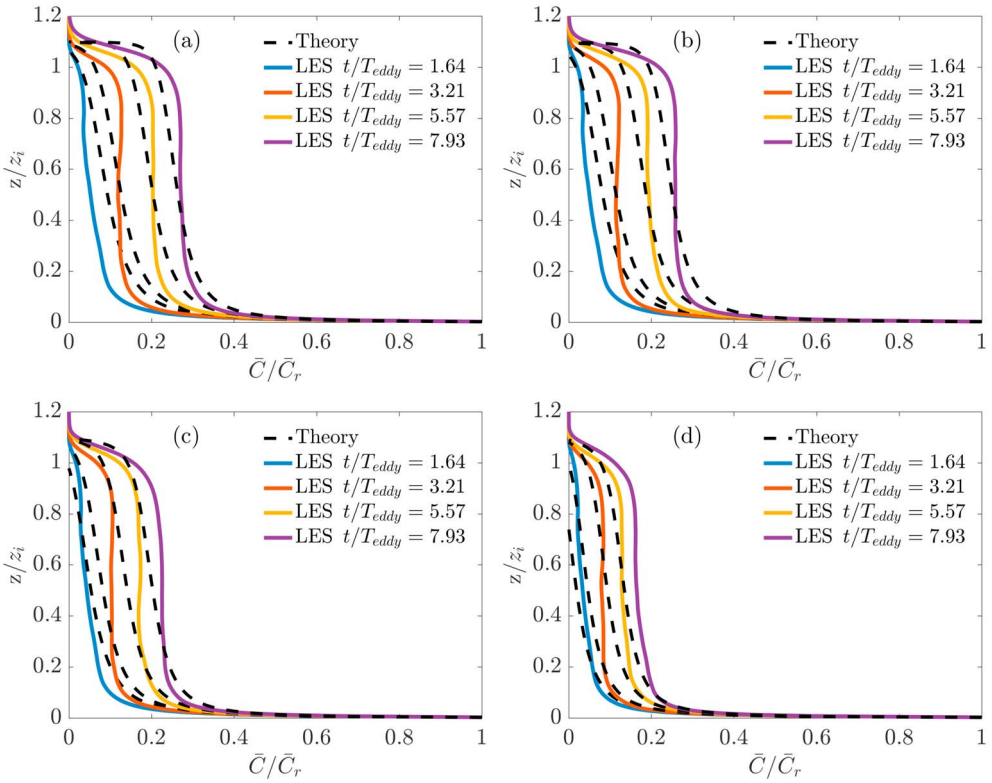

Figure 5. Comparison of normalized mean vertical concentration profile with large eddy simulation (LES) results for case Un-S: (a) 1-μm particles, (b) 10-μm particles, (c) 20-μm particles, and (d) 30-μm particles. $\bar{C}_r$ is taken as the concentration at the first vertical grid point from the LES simulation (1.56 m).

gravitational settling) in the surface layer is acceptable when calculating the mean concentration profile, even before stationarity of the concentration is reached throughout the full boundary layer.

Figure 4 shows the comparisons of normalized mean concentration profiles for the full MABL for case N at different times. All of the time stamps in the figure represent the time after the start of particle emission. When compared throughout the full boundary layer, at early times the model calculations deviate from the simulations results, while the comparison between the theory and the LES results agree well at later times. The reason for this difference is that the assumption of a linear net vertical flux from surface to inversion layer height is not accurate at early time periods, as shown in Figure 2a. At the beginning stages of the development, particles are not completely mixed throughout the MABL and thus the particle flux has not fully extended up to the inversion layer height—this transient period is not considered in the theoretical model formulation. However, once the particles are completely mixed to the top of the MABL, the model gives a reasonable approximation for the mean concentration profile. Furthermore, by comparing mean concentration profiles for different particle sizes (Figures 4a–4d), it can be observed that the concentration profile significantly changes with particle size for the same flow conditions due to gravitational settling.

Figure 5 presents the normalized mean concentration profiles for case Un-S for four different particle sizes ranging from 1 to 30 μm. As can be seen from Figures 5a–5d, the new model predicts the concentration profile with a reasonable accuracy for all tested particle sizes. While Figure 2 indicates that the linear profile given in equation (14) provides a good approximation for the net vertical flux after a single eddy turnover time, Figure 5 shows that the development of a concentration profile that is well predicted by the theory takes more like $3T_{eddy}$ to establish.

In Figure 5, a comparison between the model and the LES results shows that the model, while approximating the overall shape of the concentration profile well, cannot reproduce the near-vertical gradients of $\bar{C}$ with height. This is a well-known deficiency of K theory in unstable stratification (e.g., ; Wyngaard, 2010), where mixing is nonlocal and expressing turbulent fluxes via a gradient diffusion hypothesis is not entirely accurate. In reality, large eddies or plumes are carrying scalars vertically across the boundary layer, especially in unsta-

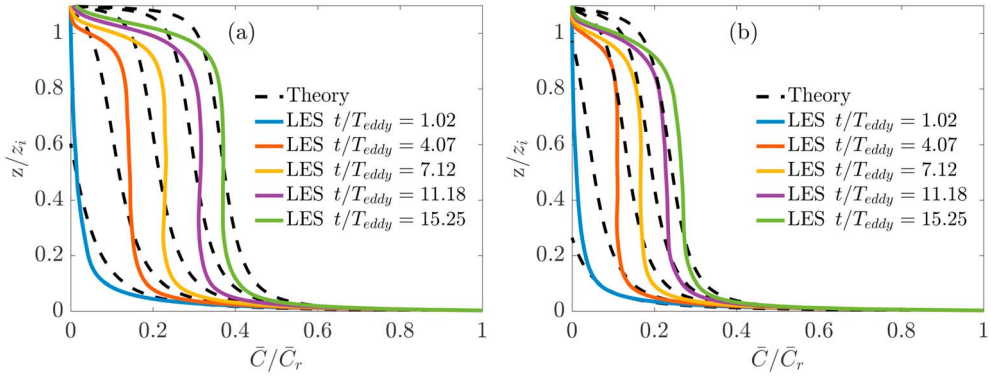

Figure 6. Comparison of normalized mean vertical concentration profile with LES results for case Un-W: (a) 10-μm particles and (b) 20-μm particles. $\bar{C}_r$ is taken as the concentration at the first vertical grid point from the LES simulation (1.56 m).

ble conditions (Shpund et al., 2011). Hence, under very unstable conditions, we expect the theory to produce vertical gradients of concentration, which are too low (i.e., not near infinite, as shown in Figure 5). Therefore, the theory consistently underpredicts the gradient $\frac{\partial \bar{C}}{\partial z}$ in the center region of the boundary layer. Nonetheless, the overall shape and behavior of $\bar{C}(z)$ is captured well by the theory and improvements of K_c, including nonlocal approximations and/or improvements to the stability function $\phi_c(\zeta)$ in the upper regions of the MABL, would be necessary to overcome this limitation.

By comparing cases N and Un-S (Figures 4 and 5, respectively), a question emerges as to how well the theory would perform for weakly unstable stratification; that is, is the transition between the relatively long transient period of neutral stratification to the relatively fast agreement between the theory and LES of strongly unstable stratification smooth or abrupt? Figure 3 suggests that a key assumption behind the current theory, that of a linear flux with height, only requires a small amount of vertical mixing to be a decent approximation. Figure 6 demonstrates that although this transition appears abrupt (only two particle sizes are shown for brevity), the development of a concentration profile that is well predicted by the theory is still limited by an initial transient period discussed above.

Finally, while Figures 4–6 show the vertical distribution of particles for various sizes and atmospheric stability, a quantity often desired in meteorological or remote sensing applications is the total mass loading in the entire boundary layer. As the concentration profile evolves in time, Figures 7–9 show the total integrated particle loading as predicted by the LES and the model for the neutral, strongly unstable, and weakly unstable cases, respectively. Only results from the 10- and 20-μm cases are shown but are illustrative of the overall behavior. Note that for the LES, the constant prescribed net surface flux of $\Phi = 0.2\ \mu g \cdot m^{-2} \cdot s^{-1}$ means that the total mass loading will increase linearly in time.

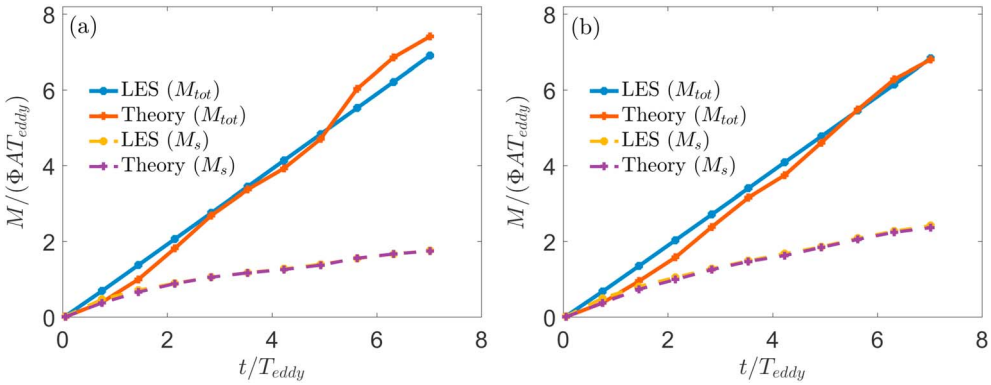

Figure 7. Comparison of total aerosol mass loading with large eddy simulation (LES) results for case N: (a) 10-μm particles and (b) 20-μm particles. M_{tot} and M_s are the total integrated particle loading in the marine atmospheric boundary layer and in the surface layer, respectively, which are normalized by $\Phi A T_{eddy}$, where A is the total horizontal area of the domain.

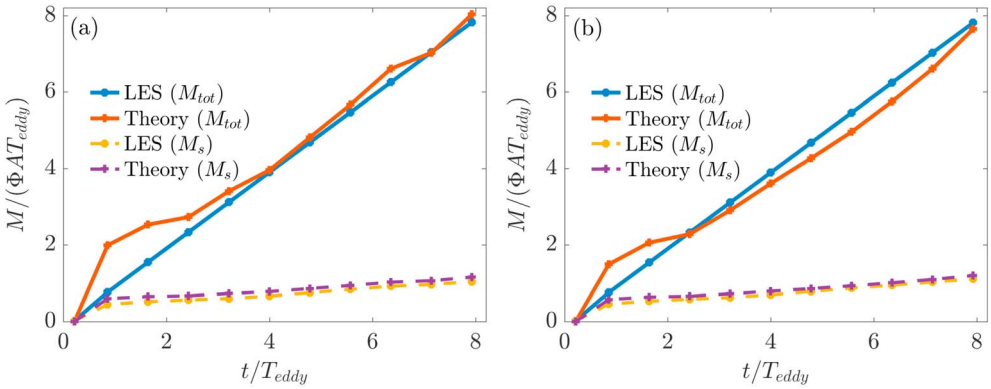

Figure 8. Comparison of total aerosol mass loading with large eddy simulation (LES) results for case Un-S: (a) 10-μm particles and (b) 20-μm particles.

For neutral stability, Figure 7 demonstrates that although the details of the profile $\bar{C}(z)$ can deviate between the theory and LES, particularly at early times and toward the top of the boundary layer, these errors are small in terms of the total loading. Even at early times, the total mass loading predicted by the theory tracks that which is predicted by the LES. This is consistent with the idea that the surface layer contains a significant fraction of the total loading (as depicted in Figure 7) and quickly approaches an approximate equilibrium balance between settling and turbulent transport.

For unstable stratification, however, the presence of an initial overprediction or underprediction of the actual mass loading is apparent for both cases Un-S and Un-W, respectively. As noted above, this initial transient adjustment takes approximately three eddy turnover times for both case Un-S (Figure 8) and case Un-W (Figure 9), somewhat depending on particle size.

4.3. Analytic Expression

As discussed above, equation (12) does not permit a closed-form analytic solution in the mixed layer for the assumed eddy diffusivity. For the neutral stability, however, we can formulate a partially closed solution, which is useful in understanding the importance of different terms in the equation. Given an expression for the eddy diffusivity, which is a piecewise continuous function of height z (equation (11), the analytic solution for the mean concentration is also a piecewise continuous function given by

$$\frac{\bar{C}}{\bar{C}_r} = \left[1 + \frac{\Phi}{w_s \bar{C}_r} - \frac{\beta z_r}{\kappa u_* (\gamma + 1)\bar{C}_r}\right]\left(\frac{z}{z_r}\right)^{-\gamma} - \frac{\Phi}{w_s \bar{C}_r} + \frac{\beta z}{\kappa u_* (\gamma + 1)\bar{C}_r}; \qquad z \le z_b \tag{15}$$

$$\frac{\bar{C}}{\bar{C}_b} = \left[1 + \frac{\Phi}{w_s \bar{C}_b} - \frac{\beta l(z)}{\mu(z)\bar{C}_b}\bigg|_{z_b}\right]\left(\frac{z}{z_b}\right)^{-\gamma}\left(\frac{z - z_i}{z_b - z_i}\right)^{\gamma} - \frac{\Phi}{w_s \bar{C}_b} + \frac{\beta l(z)}{\mu(z)\bar{C}_b}; \qquad z > z_b \tag{16}$$

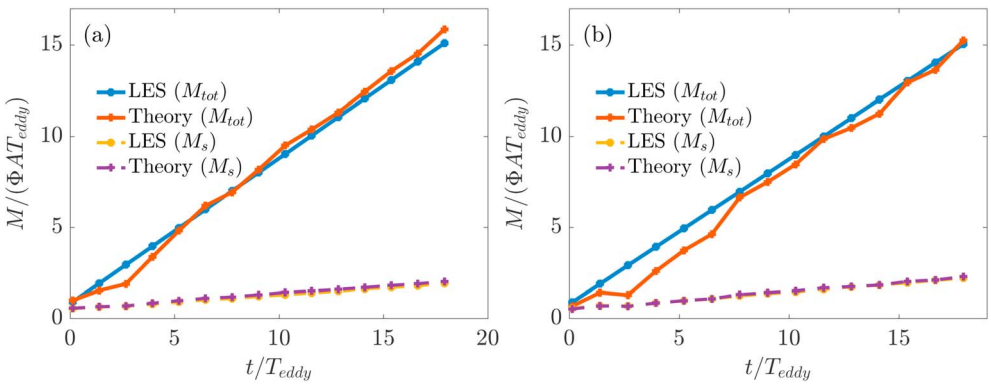

Figure 9. Comparison of total aerosol mass loading with large eddy simulation (LES) results for case Un-W: (a) 10-μm particles and (b) 20-μm particles.

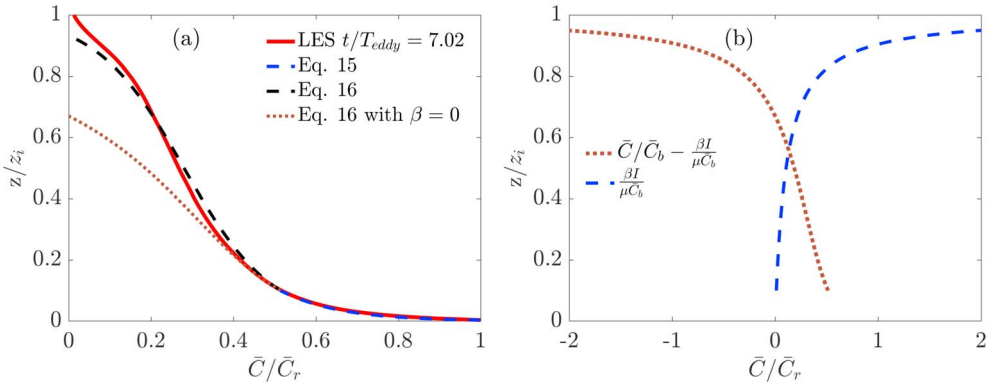

Figure 10. Analytic profile for normalized mean vertical concentration for case N with 1-μm particles: (a) comparison with large eddy simulation (LES) simulations and (b) comparison of the $\frac{\beta I(z)}{\mu(z)\bar{C}_b}$ term with the rest of equation (16).

The first of these expressions is closed, and in the second the term $I(z)$ refers to the integral given by

$$I(z) = \int \frac{z_i^2}{a\kappa u_*} \frac{z^\gamma}{(z_i - z)^{\gamma+2}} e^{\frac{\gamma}{1-z/z_i}} dz, \tag{17}$$

and the term $\mu(z)$ is given by

$$\mu(z) = \left(\frac{z}{z_i - z}\right)^\gamma e^{\frac{\gamma}{1-z/z_i}}. \tag{18}$$

$\bar{C}_b$ is the mean concentration at $z = z_b$ calculated from equation (15).

The integral $I(z)$ does not have an analytic solution, and therefore, the term $\frac{\beta I(z)}{\mu(z)\bar{C}_b}$ in equation (16) must be calculated numerically. The term $\left[\frac{\beta I(z)}{\mu(z)\bar{C}_b}\right]_{z_b}$ is a numerical constant evaluated at z_b. Both of these terms in equation (16), which prevent a closed-form solution, contain β, which comes from the linear correction to the net vertical flux. Therefore, in the limit of $\beta = 0$, which refers to a steady concentration $\frac{\partial \bar{C}}{\partial t} = 0$ (or, equivalently, a uniform vertical flux throughout the MABL), one can recover an analytic expression for the concentration in neutral stability since the terms that contain $I(z)$ drop out.

Figure 10a compares the LES profiles with 1-μm particles in neutral stability to equations (15) and (16), calculating $I(z)$ numerically (this is identical to solving equation (12) numerically). As noted above, these profiles match very closely the LES results. Also included is the solution for $\beta = 0$, for which there is a closed-form solution. This approximation, however, illustrates that the time variation of $\bar{C}$ in the MABL, and the consequent linear variation of the total concentration flux, are critical for obtaining an accurate model for $\bar{C}(z)$. Figure 10b confirms this, by comparing directly the term $\frac{\beta I(z)}{\mu(z)\bar{C}_b}$ with the rest of expression (16). Near the surface, the approximation of $\beta = 0$ is justified, as seen above in comparisons of $\bar{C}(z)$ in the surface layer. In the upper levels of the MABL, however, the term involving $I(z)$ actually dominates the solution, thus necessitating a numerical approximation for the proposed model.

5. Conclusions

In this paper we present a new theoretical model to calculate the mean vertical concentration of aerosols in the MABL. The proposed model extends the conventional surface layer similarity theories to the full atmospheric boundary layer based on a conventional treatment of turbulent diffusion. The model accounts for atmospheric stability, gravitational settling, a nonzero net surface flux, and unsteadiness when calculating the vertical concentration profile, and thus, it is expected to work in a wide range of particle sizes. In the limit of vanishing settling velocity the model would recover predictions for passive scalars. However, large particle sizes are fundamentally limited by the near-surface effects such as inertia or waves. The model requires a prescribed net surface flux as an input to calculate the mean vertical profile, which can in principle be obtained using any sea spray generation function, which itself accounts for any wind speed and/or wave state dependence (Lenain & Melville, 2017; Ovadnevaite et al., 2014). Near the surface, wave-induced modulations to

turbulence in the boundary layer could also play a role not captured by the current theory (Buckley & Veron, 2016), and this is a topic of continued research.

In the absence of comprehensive observations of size-resolved vertical concentration, here we use LES to validate the model. The validation uses four different particle diameters ranging from 1 to 30 μm and both neutral and unstable conditions. The LES simulations are designed to represent the particle emission from a uniform surface source, and the resulting mean vertical concentrations are compared with the new model. The model comparisons showed good agreement for both neutral and unstable atmospheric boundary layers for the tested range of droplet diameters. Further, the model produced consistent results with existing surface layer similarity models if applied only in the surface layer. In neutral stability conditions, the mean concentration profiles showed a strong dependency on particle size, while under unstable atmospheric stability concentration profiles are more influenced by atmospheric turbulence, as expected. However, for larger droplets (30 μm) or in weakly unstable condition both gravity and atmospheric stability were important and should be included in the model. The results showed that the assumption of a linear net vertical flux profile in the mixed layer is essential for accurate prediction of concentration above the surface layer.

The developed theoretical model can be used to calculate aerosol concentration profiles in the MABL for a wide range of applications, particularly where the boundary layer is not fully resolved. It is particularly accurate at predicting the total aerosol loading in addition to its vertical distribution. Although the focus of this paper in on sea spray aerosols, the developed model can be used for other types of aerosols such as dust or sand particles.

Acknowledgments
I. N., H. P., and D. R. were supported by the Office of Naval Research (ONR) under Grant N00014-16-1-2472. M. C. was supported by NSF Grant AGS-1358593. L. F. was funded by the Brazilian National Council for Scientific and Technological Development (CNPq-Brazil). J. R. was supported by NRL base program and ONR 322. The authors would like to thank the Computing Research Center at the University of Notre Dame for computational support. Data presented in this work can be found at doi:10.7274/R0HX19SC

References

Andreas, E. L. (1998). A new sea spray generation function for wind speeds up to 32 m s^{-1}. *Journal of Physical Oceanography*, *28*(11), 2175–2184.
Andreas, E. L., Edson, J. B., Monahan, E. C., Rouault, M. P., & Smith, S. D. (1995). The spray contribution to net evaporation from the sea: A review of recent progress. *Boundary Layer Meteorology*, *72*, 3–52.
Andreas, E. L., Jones, K. F., & Fairall, C. W. (2010). Production velocity of sea spray droplets. *Journal of Geophysical Research*, *115*, C12065. https://doi.org/10.1029/2010JC006458
Balachandar, S., & Eaton, J. K. (2010). Turbulent dispersed multiphase flow. *Annual Review of Fluid Mechanics*, *42*, 111–133.
Blanchard, D. C., Woodcock, A. H., & Cipriano, R. J. (1984). The vertical distribution of the concentration of sea salt in the marine atmosphere near Hawaii. *Tellus B*, *36*(2), 118–125.
Bou-Zeid, E., Meneveau, C., & Parlange, M. (2005). A scale-dependent lagrangian dynamic model for large eddy simulation of complex turbulent flows. *Physics of fluids*, *17*(2), 025105.
Brost, R. A., & Wyngaard, J. C. (1978). A model study of the stably stratified planetary boundary layer. *Journal of the Atmospheric Sciences*, *35*(8), 1427–1440.
Buckley, M. P., & Veron, F. (2016). Structure of the airflow above surface waves. *Journal of Physical Oceanography*, *46*(5), 1377–1397.
Chamberlain, A. C. (1967). Transport of Lycopodium spores and other small particles to rough surfaces. *Proceedings of the Royal Society A: Mathematical, Physical and Engineering Sciences*, *296*(444), 45–70.
Chamecki, M., & Meneveau, C. (2011). Particle boundary layer above and downstream of an area source: Scaling, simulations, and pollen transport. *Journal of Fluid Mechanics*, *683*, 1–26.
Chamecki, M., Meneveau, C., & Parlange, M. B. (2009). Large eddy simulation of pollen transport in the atmospheric boundary layer. *Journal of Aerosol Science*, *40*, 241–255.
Chamecki, M., van Hout, R., Meneveau, C., & Parlange, M. B. (2007). Concentration profiles of particles settling in the neutral and stratified atmospheric boundary layer. *Boundary Layer Meteorology*, *125*(1), 25.
de Leeuw, G. (1986). Vertical profiles of giant particles close above the sea surface. *Tellus*, *38B*, 51–61.
de Leeuw, G., Andreas, E. L., Anguelova, M. D., Fairall, C. W., Lewis, E. R., O'Dowd, C. D., et al. (2011). Production flux of sea spray aerosol. *Reviews of Geophysics*, *49*, RG2001. https://doi.org/10.1029/2010RG000349
Estoque, M. A. (1963). A numerical model of the atmospheric boundary layer. *Journal of Geophysical Research*, *68*(4), 1103–1113.
Fairall, C. W., Banner, M. L., Peirson, W. L., Asher, W., & Morison, R. P. (2009). Investigation of the physical scaling of sea spray spume droplet production. *Journal of Geophysical Research*, *114*, C10001. https://doi.org/10.1029/2008JC004918
Fairall, C. W., Pezoa, S., Moran, K., & Wolfe, D. (2014). An observation of sea-spray microphysics by airborne Doppler radar. *Geophysical Research Letters*, *41*, 3658–3665. https://doi.org/10.1002/2014GL060062
Freire, L. S., Chamecki, M., & Gillies, J. A. (2016). Flux-profile relationship for dust concentration in the stratified atmospheric surface layer. *Boundary Layer Meteorology*, *160*(2), 249–267.
Holtslag, A. A. M., & Moeng, C.-H. (1991). Eddy diffusivity and countergradient transport in the convective atmospheric boundary layer. *Journal of the Atmospheric Sciences*, *48*(14), 1690–1698.
Hoppel, W. A., Frick, G. M., & Fitzgerald, J. W. (2002). Surface source function for sea-salt aerosol and aerosol dry deposition to the ocean surface. *Journal of Geophysical Research*, *107*(D19), 4382.
Kaimal, J. C., & Finnigan, J. J. (1994). *Atmospheric boundary layer flows: Their structure and measurement*. New York, Oxford: Oxford University Press.
Kind, R. J. (1992). One-dimensional aeolian suspension above beds of loose particles- a new concentration-profile equation. *Atmospheric Environment. Part A. General Topics*, *26*(5), 927–931.
Kleefeld, C., O'Dowd, C. D., O'Reilly, S., Jennings, S. G., Aalto, P., Becker, E., et al. (2002). Relative contribution of submicron and supermicron particles to aerosol light scattering in the marine boundary layer. *Journal of Geophysical Research*, *107*(D19), 8103.
Kumar, V., Kleissl, J., Meneveau, C., & Parlange, M. B. (2006). Large-eddy simulation of a diurnal cycle of the atmospheric boundary layer: Atmospheric stability and scaling issues. *Water Resources Research*, *42*(6), W06D09. https://doi.org/10.1029/2005WR004651

Lenain, L., & Melville, W. K. (2017). Evidence of sea-state dependence of aerosol concentration in the marine atmospheric boundary layer. *Journal of Physical Oceanography*, *47*(1), 69–84.
Lewis, E. R., & Schwartz, S. E. (2004). *Sea salt aerosol production: Mechanisms, methods, measurements, and models—A critical review*. Washington, DC: American Geophysical Union.
Maxey, M. R. (1987). The gravitational settling of aerosol particles in homogeneous turbulence and random flow fields. *Journal of Fluid Mechanics*, *174*, 441–465.
McPherson, R. D. (1968). A three-dimension numerical study of the Texas coast sea breeze, (PhD thesis). University of Texas at Austin.
Moeng, C.-H. (1984). A large-eddy-simulation model for the study of planetary boundary-layer turbulence. *Journal of the Atmospheric Sciences*, *41*(13), 2052–2062.
Moeng, C.-H., & Sullivan, P. P. (1994). A comparison of shear- and buoyancy-driven planetary boundary layer flows. *Journal of the Atmospheric Sciences*, *51*(7), 999–1022.
Moeng, C.-H., & Wyngaard, J. C. (1984). Statistics of conservative scalars in the convective boundary layer. *Journal of the Atmospheric Sciences*, *41*(21), 3161–3169.
Monin, A. S., & Yaglom, A. M. (1971). *Statistical Fluid Mechanics*, (Vol. I and II). Cambridge: MIT Press.
Mueller, J. A., & Veron, F. (2009). A Lagrangian stochastic model for heavy particle dispersion in the atmospheric marine boundary layer. *Boundary Layer Meteorology*, *130*(2), 229–247.
Mueller, J., & Veron, F. (2010). A Lagrangian stochastic model for sea-spray evaporation in the atmospheric marine boundary layer. *Boundary Layer Meteorology*, *137*(1), 135–152.
Norris, S. J., Brooks, I. M., Moat, B. I., Yelland, M., de Leeuw, G., Pascal, R. W., & Brooks, B. (2013). Near-surface measurements of sea spray aerosol production over whitecaps in the open ocean. *Ocean Science*, *9*, 133–145.
O'Brien, J. J. (1970). A note on the vertical structure of the eddy exchange coefficient in the planetary boundary layer. *Journal of the Atmospheric Sciences*, *27*(8), 1213–1215.
O'Dowd, C., & De Leeuw, G. (2007). Marine aerosol production: A review of the current knowledge. *Philosophical Transactions of the Royal Society of London A: Mathematical, Physical and Engineering Sciences*, *365*(1856), 1753–1774.
Ovadnevaite, J., de Leeuw, G., Ceburnis, D., Monahan, C., Partanen, A.-I., Korhonen, H., et al. (2014). A sea spray aerosol flux parameterization encapsulating wave state. *Atmospheric Chemistry and Physics*, *14*(4), 1837.
Pan, Y., Chamecki, M., & Isard, S. A. (2013). Dispersion of heavy particles emitted from area sources in the unstable atmospheric boundary layer. *Boundary Layer Meteorology*, *146*(2), 235–256.
Peng, T., & Richter, D. (2017). Influence of evaporating droplets in the turbulent marine atmospheric boundary layer. *Boundary Layer Meteorology*, *165*(3), 497–518.
Porté-Agel, F. (2004). A scale-dependent dynamic model for scalar transport in large-eddy simulations of the atmospheric boundary layer. *Boundary Layer Meteorology*, *112*(1), 81–105.
Prandtl, L. (1953). Essentials of fluid dynamics: With applications to hydraulics, aeronautics, meteorology and other subjects.
Reid, J. S., Brooks, B., Crahan, K. K., Hegg, D. A., Eck, T. F., O'Neill, N., et al. (2006). Reconciliation of coarse mode sea-salt aerosol particle size measurements and parameterizations at a subtropical ocean receptor site. *Journal of Geophysical Research*, *111*, D02202. https://doi.org/10.1029/2005JD006200
Reid, J. S., Jonsson, H. H., Smith, M. H., & Smirnov, A. (2001). Evolution of the vertical profile and flux of large sea-salt particles in a coastal zone. *Journal of Geophysical Research*, *106*(D11), 12,039–12,053.
Richter, D. H., & Chamecki, M. (2018). Inertial effects on the vertical transport of suspended particles in a turbulent boundary layer. *Boundary Layer Meteorology*, *167*, 235–256. https://doi.org/10.1007/s10546-017-0325-3
Rouse, H. (1937). Modern conceptions of the mechanics of fluid turbulence. *American Society of Civil Engineers Transactions*, *102*, 463–505.
Seinfeld, J. H., & Pandis, S. N. (1998). *Atmospheric chemistry and physics: From air pollution to climate*. New York: Wiley.
Shao, Y. (2000). *Physics and modelling of wind erosion (Atmospheric and Oceanographic Sciences Library)*. Dordrecht, Netherlands: Klewer Academic Publishers.
Shpund, J., Pinsky, M., & Khain, A. (2011). Microphysical structure of the marine boundary layer under strong wind and spray formation as seen from simulations using a 2D explicit microphysical model. Part I: The impact of large eddies. *Journal of the Atmospheric Sciences*, *68*(10), 2366–2384.
Smith, M. H., Park, P. M., & Consterdine, IE (1993). Marine aerosol concentrations and estimated fluxes over the sea. *Quarterly Journal of the Royal Meteorological Society*, *119*(512), 809–824.
Troen, I. B., & Mahrt, L. (1986). A simple model of the atmospheric boundary layer: Sensitivity to surface evaporation. *Boundary Layer Meteorology*, *37*(1-2), 129–148.
Twohy, C. H., Petters, M. D., Snider, J. R., Stevens, B., Tahnk, W., Wetzel, M., et al. (2005). Evaluation of the aerosol indirect effect in marine stratocumulus clouds: Droplet number, size, liquid water path, and radiative impact. *Journal of Geophysical Research*, *110*, D08203. https://doi.org/10.1029/2004JD005116
Veron, F. (2015). Ocean spray. *Annual Review of Fluid Mechanics*, *47*, 507–538.
Waggy, S. B., Biringen, S., & Sullivan, P. P. (2013). Direct numerical simulation of top-down and bottom-up diffusion in the convective boundary layer. *Journal of Fluid Mechanics*, *724*, 581–606.
Weil, J. C. (1990). A diagnosis of the asymmetry in top-down and bottom-up diffusion using a Lagrangian stochastic model. *Journal of the Atmospheric Sciences*, *47*(4), 501–515.
Weil, J. C., Sullivan, P. P., & Moeng, C.-H. (2004). The use of large-eddy simulations in Lagrangian particle dispersion models. *Journal of the Atmospheric Sciences*, *61*(23), 2877–2887.
Wyngaard, J. C. (2010). *Turbulence in the atmosphere*. Cambridge: Cambridge University Press.
Wyngaard, J. C., & Brost, R. A. (1984). Top-down and bottom-up diffusion of a scalar in the convective boundary layer. *Journal of the Atmospheric Sciences*, *41*(1), 102–112.
Xiao, J., & Taylor, P. A. (2002). On equilibrium profiles of suspended particles. *Boundary-Layer Meteorology*, *105*(3), 471–482.
Zhu, Z., Hu, R., Zheng, X., & Wang, Y. (2017). On dust concentration profile above an area source in a neutral atmospheric surface layer. *Environmental Fluid Mechanics*, *17*(6), 1171–1188.